Pergamon

Int. J. Heat Mass Transfer. Vol. 37, No. 6, pp. 917–925, 1994

0017–9310/94 $6.00 + 0.00

0017–9310(93)E0013–7

A study of natural convection heat transfer in a vertical rectangular enclosure with two-dimensional discrete heating: effect of aspect ratio

C. J. HO† and J. Y. CHANG

Department of Mechanical Engineering, National Cheng Kung University, Tainan, Taiwan 701, R.O.C.

(*Received* 4 *March* 1993 *and in final form* 18 *October* 1993)

Abstract—Natural convection heat transfer inside a vertical rectangular enclosure with four two-dimensional discrete flush-mounted heaters is investigated numerically and experimentally to unveil primarily the influence of aspect ratio of the enclosure. Numerical simulations for the problem have been conducted for the aspect ratio varying from 1 to 10 and the modified Rayleigh number in the range between 10^3 and 10^7 with a given relative heater size and location. Numerical results reveal that the increase of the aspect ratio leads to substantial degradation of convective dissipation from the discrete heaters. The highest heater surface temperature occurs usually at the top heater for $Ra^* \geqslant 10^4$ regardless the aspect ratio of enclosure. Correlation in terms of the modified Rayleigh number and the aspect ratio of the enclosure has been generated for the average Nusselt numbers for each heater as well as the maximum surface temperature at the discrete heaters. Holographic interferometry and a smoke flow visualization are employed to map the temperature and flow fields within an enclosure of aspect ratio 10. The predicted temperature and flow fields are found to be in good agreement with the experiments.

INTRODUCTION

THIS PAPER presents a combined numerical and experimental study treating the natural convection cooling of discrete flush-mounted heaters inside a vertical rectangular enclosure, as illustrated schematically in Fig. 1. Due to its high reliability, absence of noise, freedom from electromagnetic interference, and low maintenance cost, natural convection has been considered as a preferred heat transfer mechanism in electronic equipment cooling. Comprehensive reviews of natural convection electronic cooling are available [1, 2]. Under certain circumstances, such as operation of electronic equipment in dusty or hazardous environment, electronic components are packaged within sealed enclosures. The components may be mounted to one vertical wall of the enclosure, while one or more of the other walls is cooled, as the physical configuration considered in the present study.

Following the pioneering numerical work of Chu *et al.* [3] on two-dimensional, laminar natural convection cooling of a single, isothermal flush-mounted heater on a vertical wall inside an air-filled rectangular enclosure, the heat transfer problem of natural convection in a discretely heated enclosure is of great research interest as indicated by the considerable research activities on this subject. A natural convection heat transfer experiment in a tall vertical rectangular enclosure (aspect ratio 16.5) with an array of eleven discrete flush-heaters has been performed by Keyhani *et al.* [4]. It was found that the discrete heating in the enclosure results in a significantly augmented local heat transfer rate over that for an enclosure with the uniformly heated vertical wall. A follow-up study [5] for a vertical enclosure aspect ratio 4.5 with three flush heaters further revealed that the temperature of the heaters is strongly affected by the stratification of fluid inside the enclosure. Moreover, the effects of enclosure width and Prandtl number on natural convection liquid cooling of discrete flush heaters in a tall enclosure cooled from the top has been investigated experimentally and numerically [6–7]. More recently, Refai Ahmed and Yovanovich [8] performed a numerical study to examine the influence of discrete heat source location on natural convection heat transfer in a vertical square enclosure. Furthermore, the temperature field of natural convection within a discretely heated vertical enclosure with single and dual heaters configuration has been visualized using Mach–Zehnder interferometry [9]. Two-dimensional numerical simulations were also carried out for a tall vertical rectangular enclosure of aspect ratio 5 with three, four, or five discrete heat sources. The results further confirmed that the heater location yielding the maximum heat transfer was also a function of Grashof number.

In addition, experiments [10, 11] and numerical simulations [12, 13] have been reported on natural convection in rectangular enclosures with discretely heated protrusions on one vertical wall. Results from these studies revealed that the buoyancy-driven flow was concentrated in the gap region between the protruding heaters.

† Author to whom the correspondence should be addressed.

NOMENCLATURE

a	coefficient
A	surface area
AR	aspect ratio, H/W
b, c	exponents
g	gravitational acceleration
h	heat transfer coefficient
H	height of enclosure
k	thermal conductivity
l	heater length
L	dimensionless heater length, l/W
Nu	Nusselt number
Pr	Prandtl number
q	heat flux
Q	electric power or heat transfer rate
Ra^*	modified Rayleigh number, $g\beta q_h W^4/(k\nu\alpha)$
s	spacing between discrete heaters
T	temperature
W	width of enclosure
x^+, y^+	Cartesian coordinates
x, y	dimensionless coordinates, $x^+/W, y^+/W$.

Greek symbols

α	thermal diffusivity
β	thermal expansion coefficient
θ	dimensionless temperature, $k(T-T_c)/(q_h W)$
ν	kinematic viscosity
ψ^+	stream function
ψ	dimensionless stream function, ψ^+/α
ω^+	vorticity
ω	dimensionless vorticity, $\omega^+ W^2/\alpha$.

Subscripts

c	cold wall
h	heater wall
l	heat loss
max	maximum value
rad	radiation component.

Superscript

$\bar{}$	surface averaged value.

The present study represents a continuing effort to supplement the earlier studies with numerical simulations and experimental data of natural convection air cooling of an array of two-dimensional discrete flush heaters on a vertical wall of a rectangular enclosure. Specifically, the primary objective of this study is to examine systematically the effect of the enclosure aspect ratio on the heat transfer characteristics of natural convection due to four equally-spaced discrete heat sources on a vertical wall of a rectangular enclosure.

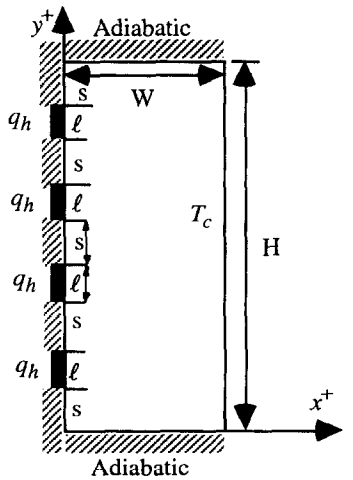

FIG. 1. Schematic diagram of physical configuration and coordinate system.

MATHEMATICAL FORMULATION AND NUMERICAL METHOD

For the physical configuration shown in Fig. 1, the two-dimensional steady, laminar natural convection heat transfer in an air-filled, vertical rectangular enclosure with four discrete flush-mounted heat sources of isoflux q_h on the left vertical wall is considered. The discrete heaters of length l are placed at an equal spacing s between the fixed adiabatic top and bottom surfaces of the enclosure. The right vertical wall of the enclosure is isothermally cooled at temperature T_c. The fluid (air) within the enclosure is assumed to be Newtonian adhering to the Boussinesq approximation. The conservation for the mass, momentum, and energy governing the buoyancy-driven fluid flow and heat transfer in the enclosure may then be formulated in terms of dimensionless quantities of stream function, vorticity, and temperature, respectively, as follows:

$$\frac{\partial^2\psi}{\partial x^2}+\frac{\partial^2\psi}{\partial y^2}=-\omega \tag{1}$$

$$\frac{\partial\psi}{\partial y}\frac{\partial\omega}{\partial x}-\frac{\partial\psi}{\partial x}\frac{\partial\omega}{\partial y}=Pr\left(\frac{\partial^2\omega}{\partial x^2}+\frac{\partial^2\omega}{\partial y^2}\right)+Pr\,Ra^*\frac{\partial\theta}{\partial x} \tag{2}$$

$$\frac{\partial\psi}{\partial y}\frac{\partial\theta}{\partial x}-\frac{\partial\psi}{\partial x}\frac{\partial\theta}{\partial y}=\frac{\partial^2\theta}{\partial x^2}+\frac{\partial^2\theta}{\partial y^2}. \tag{3}$$

The dimensionless boundary conditions for the present problem may be written as:

Table 1. Average Nusselt numbers on four discrete heaters in an air-filled rectangular enclosure of aspect ratio 5

Ra^*	$(\overline{Nu_h})_1$	$(\overline{Nu_h})_2$	$(\overline{Nu_h})_3$	$(\overline{Nu_h})_4$
7100	1.110(1.165)†	1.343(1.367)	1.591(1.687)	2.098(2.183)
71 000	1.830(1.912)	2.212(2.239)	2.685(2.767)	3.503(3.581)

† Values in the parentheses are based on the correlation of ref. [9].

$$x = 0;\quad \psi = 0,\quad \frac{\partial\theta}{\partial x} = -1 \text{ (at heaters)},$$

$$\frac{\partial\theta}{\partial x} = 0 \text{ (elsewhere)} \tag{4a}$$

$$x = 1;\quad \psi = 0,\quad \theta = 0 \tag{4b}$$

$$y = 0 \quad \text{or } AR;\quad \psi = 0,\quad \frac{\partial\theta}{\partial y} = 0. \tag{4c}$$

The local heat transfer rates at the discretely heated wall and the isothermally cold wall are, respectively, presented by means of local Nusselt numbers defined as follows:

$$Nu_h = \frac{1}{\theta_h} \tag{5a}$$

and

$$Nu_c = -\left.\frac{\partial\theta}{\partial x}\right|_{x=1}. \tag{5b}$$

Numerical solutions to the foregoing governing differential equations for the present problem were obtained via a finite difference method. The finite difference discretization schemes and the solution methodology employed in the present work basically follow those described in ref. [14], thus obviating the need to further elaborate here. The computer code of the present study was validated by performing calculations for natural convection inside an air-filled rectangular enclosure of aspect ratio of 1 and 10. The computed values of the heat transfer results and the stream function extreme were found to be in good agreement with the corresponding results of de Vahl Davis [15] and Ramman and Korpela [16], respectively. Further validation of the numerical algorithm adopted in the present study was carried out for natural convection in an air-filled vertical rectangular enclosure (aspect ratio 5) due to four discrete flush heaters like that considered in ref. [9]. As indicated in Table 1, the computed results of the average Nusselt number on the discrete heaters compare favorably with those evaluated from the correlation developed in ref. [9].

Moreover, resulting from a series of grid-size dependence calculations for the present problem, a mesh system consisting of a uniform grid of 151 in the y direction and a non uniform grid of 51 in the x direction was mainly used to generate the numerical simulations for the present problem. The non uniform mesh in the x-direction was distributed to provide sufficient resolution for the development of thermal and hydrodynamic boundary layers along the vertical walls of the enclosure. The steady-state solutions obtained were also checked for energy balance at least within 1%.

EXPERIMENT

A test cell mimicking the physical configuration shown in Fig. 1 has been designed and constructed for the experiments to verify the numerical simulations undertaken in the present study. The test cell was a rectangular enclosure of aspect ratio $AR = 10$ with the inner dimensions of 300 mm (height) by 30 mm (width) by 170 mm (depth). The right vertical wall was made of a brass plate milled with spiral channels. A constant isothermal boundary imposed on the right vertical wall was achieved by pumping thermally regulated fluid (a mixture of ethanol in water) from a constant temperature bath. Five copper–constantan thermocouples were embedded in the brass wall to monitor the surface temperature distribution. The surface temperature variation of the brass wall was found to be less than 0.3°C in all the tests. The discretely heated left vertical wall of the test cell was constructed of a composite plate in which a 1 mm thick wooden sheet was adhered to a 5 mm thick acrylic plate; and on top of the wooden sheet, a 0.01 mm thick plastic sheet was adhered to provide a smooth surface. The discrete heaters made of 0.08 mm thick stainless steel strips were adhered on the composite plate at an equal spacing of 52 mm between the heaters. The stainless steel strips were heated by passing an electric current from a d.c. power supply. The electric power dissipated in the steel strips was calculated from the product of voltage drop and current measured by a voltmeter and ammeter, respectively. The error associated with the measurement for the power dissipation was estimated to be 1.3%. Fourteen thermocouples were adhered along the discretely heated vertical surface and four of them were embedded, using a high-thermal-conductivity epoxy adhesive, beneath the strip heaters to measure the surface temperature. Furthermore, the vertical walls of the front and rear ends of the test cell were made of glass windows to enable optical visualization of temperature and flow fields. To reduce heat exchange with the laboratory environment, the test cell assembly was wrapped in styrofoam boards.

The experiments were performed by monitoring

readings of the thermocouples on the discretely heated vertical wall until steady state was reached. In addition, the temperature distribution and flow structure inside the enclosure were visualized by means of a holographic interferometry and flow visualization experiment, respectively. A real-time holographic interferometry technique the same as that described in ref. [17] was employed in the present study. Flow visualization experiments were conducted using smoke generated from a burning incense stick as the flow tracer. The cross-sectional view of the buoyancy-driven flow pattern in the mid-depth of the enclosure was visualized via a slit light source and recorded photographically using a Nikon F-4 SLR camera.

In the data reduction of the experimental results, care has been taken to account for the heat exchange of the discrete heaters with the ambient via conduction through the outer insulation as well as the radiation heat transfer from the strip heater surface to the surroundings inside the enclosure. The net convection heat flux from the discrete heaters was calculated with

$$q_h = (Q - Q_l - Q_{rad})/A_h \quad (6)$$

where Q is the electric power dissipated at each heater, Q_l is the heat loss to the laboratory ambient by conduction through the insulation layer, and Q_{rad} is the radiation component dissipated from the heater surface. In the radiation estimation, two-dimensional diffuse-gray radiation exchange analysis was performed inside the enclosure based on the measured temperature of the discrete heaters. The radiative component was estimated to account for about 12% of the input power, while the conduction loss was around 20%. Due to the unequal radiative and conductive losses for the heaters, an averaged corrected convective heat flux for the four heaters was used for evaluating the modified Rayleigh number and the dimensionless temperature. The thermophysical properties of air were evaluated at an averaged temperature of the cold wall and the highest heater surface temperature in the test. Based on the uncertainty analysis [18], the errors in the experimental data of the modified Rayleigh and Nusselt numbers were 7.3 and 8.1%, respectively.

NUMERICAL RESULTS

Numerical simulations have been conducted to elucidate the effect of enclosure aspect ratio on the natural convection air ($Pr = 0.71$) cooling of an array of four flush-heater inside a vertical rectangular enclosure by varying AR ($= 1 \sim 10$) while the relative heater size, l/H, and location, s/H, on the vertical wall are fixed at 1/30 and 13/75, respectively. The range of the modified Rayleigh number considered in the present simulation is 10^3–10^7.

Flow and temperature fields

The buoyancy-driven flow and temperature fields inside the discretely heated enclosure of various aspect ratios are illustrated by means of contour maps of streamlines and isotherms, respectively, as exemplified in Figs. 2 and 3 for two different modified Rayleigh numbers. At $Ra^* = 10^3$, as can be expected, heat of the discrete heaters is essentially dissipated via a conduction-dominated mechanism as indicated by the isotherm pattern around the discrete heaters shown in Fig. 2. With increase of the aspect ratio of the enclosure, the buoyant convection flow is increasingly strengthened, exhibiting a transformation from a primarily clockwise unicellular flow into a structure characterized by regularly spaced multicellular flow in the core region for $AR \geqslant 6$, as depicted by the streamlines in Fig. 2. These split core vortices are essentially in parallel with the location of the heaters on the vertical wall. With the enhanced buoyancy due to the increase of Ra^*, the core vortices tend to drift upward, resulting in coalescence of these co-rotating vortices. Meanwhile, thermal boundary layers formed along each heater as well as the stratification in the core region become increasingly distinctive with the increase of Ra^*. As a result for Ra^* beyond a certain value, for instance, for $AR = 10$ with $Ra^* \geqslant 10^6$, the flow reverts to an unicellular structure but at enhanced strength.

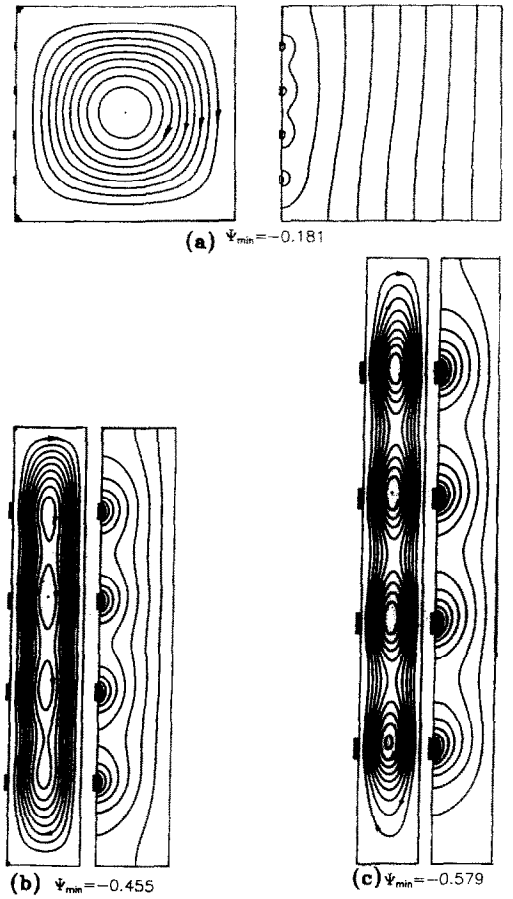

FIG. 2. Streamlines (right) and isotherms (left) for discretely heated rectangular enclosure at $Ra^* = 10^3$: (a) $AR = 1$, (b) $AR = 6$, and (c) $AR = 10$.

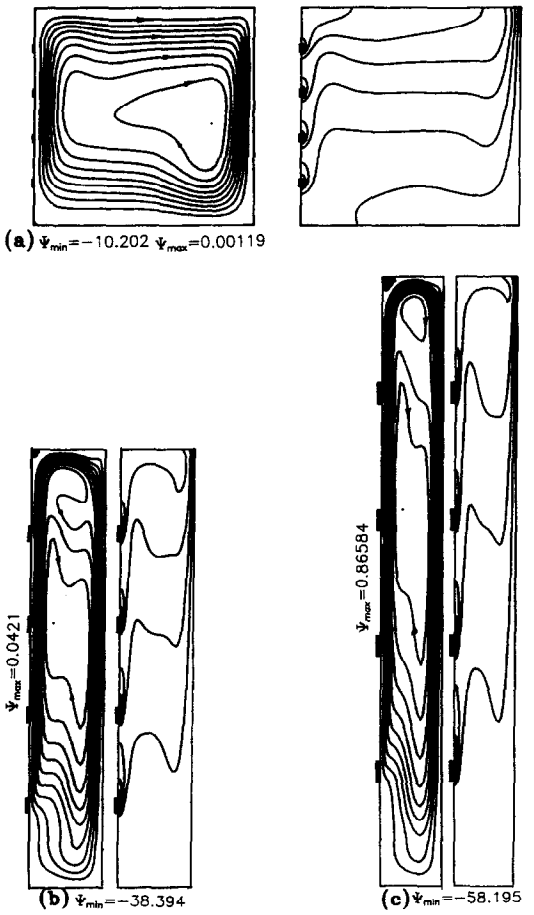

FIG. 3. Streamlines (right) and isotherms (left) for discretely heated rectangular enclosure at $Ra^* = 10^7$: (a) $AR = 1$, (b) $AR = 6$, and (c) $AR = 10$.

At $Ra^* = 10^7$, as shown in Fig. 3, the flow field persists with the unicellular structure as the aspect ratio of the enclosure increases from 1 to 10. Furthermore, the thermal structure revealed by the isotherm plots in Fig. 3 clearly indicate the dominance of convective mechanism in cooling the discrete heaters.

Typical dimensionless temperature distributions along the discretely heated vertical wall are displayed in Fig. 4 for two aspect ratios of the enclosure. From the figure it is evident that at a low modified Rayleigh number, 10^3, the four discrete heater surfaces, regardless of the aspect ratio of the enclosure, attain similar temperature variation, indicative of the dominance of conduction dissipation from the heaters. For higher modified Rayleigh number, $Ra^* \geqslant 10^4$, the increasing influence of the buoyant convection leads to increasing disparity in temperature between the discrete heaters, and a wavy temperature profile cascading over the discretely heated wall is formed. The local temperature variation over each heater starts relatively low at the leading edge and then increases sharply, reflecting development of the thermal boundary layer along each heater. The bottom heater (heater 1)

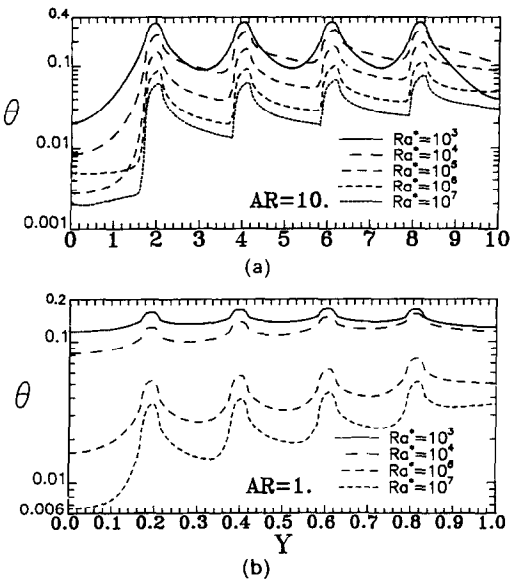

FIG. 4. Temperature profiles on the discretely heated wall at various Ra^*: (a) $AR = 10$ and (b) $AR = 1$.

has always the lowest average temperature. In ref. [9] a similar finding was reported for an enclosure ($AR = 5$) with two discrete flush-mounted heaters. Moreover, it can be inferred from Fig. 4 that the increase of modified Rayleigh number tends to reduce greatly the discrete heater temperature; while the increase of the enclosure aspect ratio gives rise to an opposite effect, yielding noticeably higher temperature on the heaters.

Another important quantity of practical interest in electronic cooling application is the maximum surface temperature (hot spot) on the discrete heater. In the present simulations, the maximum surface temperature may occur at the heater 4 (top) or heater 3, mainly depending on the modified Rayleigh number. For $Ra^* \geqslant 10^4$ the hot spot is detected at the top heater; while for $Ra^* = 10^3$ the hot spot is at the third heater. In Fig. 5, the variation of the maximum surface temperature with the aspect ratio of the enclosure is presented for different modified Rayleigh number. An overview of the figure reveals that the increase of the enclosure aspect ratio results in increasingly higher maximum surface temperatures on the heater. Further, from Fig. 5 the maximum surface temperature exhibits a strong dependence on the modified Rayleigh

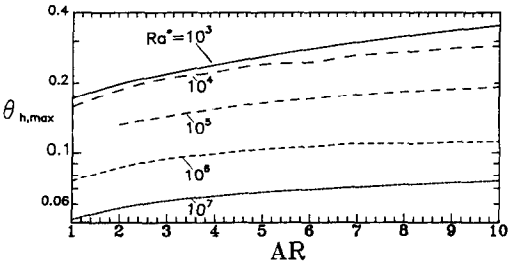

FIG. 5. Variation of the maximum heater surface temperature with the aspect ratio of the enclosure at various Ra^*.

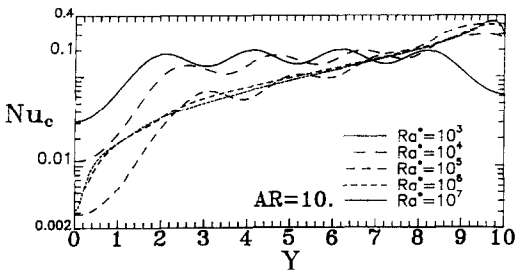

FIG. 6. Typical distribution of local Nusselt number at the isothermally cold wall of an enclosure of $AR = 10$.

number, opposite to that of increasing aspect ratio of the enclosure; namely, the increase of Ra^* produces markedly lower maximum surface temperature on the discrete heaters.

Heat transfer

Next attention is focused upon the influence of the aspect ratio on the heat transfer rate across the discretely heated enclosure. Figure 6 exemplifies distribution of the local heat transfer rate at the isothermally cold vertical wall in an enclosure of $AR = 10$. For $Ra^* = 10^3$, in conformity with the multicellular core flow illustrated in Fig. 2, the local Nusselt number features a corresponding wavy variation along the cold wall. With the reversal to unicellular flow structure resulted from increasing modified Rayleigh number, the wavy variation of the local heat transfer rate at the cold wall gradually transforms to a somewhat monotonically increasing trend from the bottom toward the top of the cold wall.

Figure 7 conveys the dependence of the average Nusselt number over each discrete heater surface on the aspect ratio of the enclosure at two values of modified Rayleigh number. For $Ra^* = 10^3$, the average Nusselt numbers on the discrete heaters tend to decrease greatly as the enclosure becomes taller. Moreover, it can be noticed that with the exception

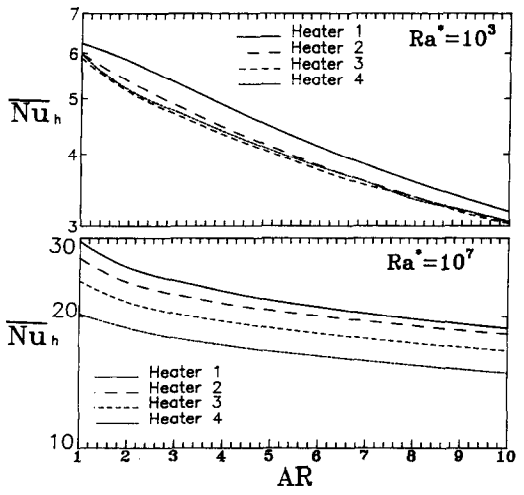

FIG. 7. Effect of aspect ratio of the enclosure on the average Nusselt number at the discretely heated wall.

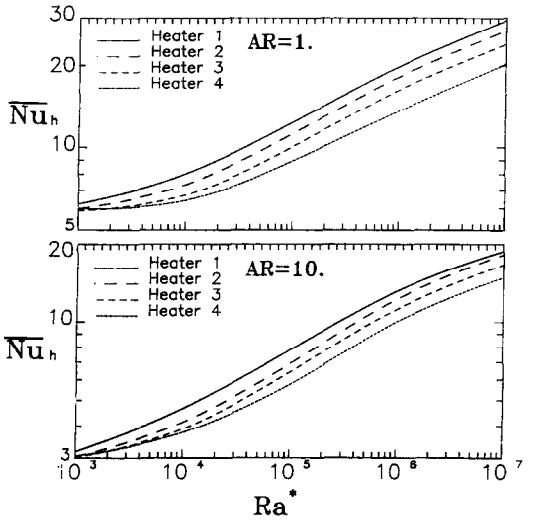

FIG. 8. Relation of the average Nusselt number with the modified Rayleigh number.

of the bottom heater, the disparity of the average Nusselt number between the remaining heaters appears to be rather minute. With the enhanced convection effect due to increasing Ra^*, the average Nusselt number difference between the four heaters becomes greatly augmented, as depicted in Fig. 7 for $Ra^* = 10^7$. Furthermore, it can be seen from the figure that the rate of decreasing average Nusselt number with increasing aspect ratio tends to drop noticeably at high modified Rayleigh number, namely, the effect of aspect ratio on the average Nusselt number on the discrete heaters is markedly degraded with the increase of Ra^*.

Moreover, the relation of the average Nusselt number of the discrete heaters with the modified Rayleigh number is exemplified in Fig. 8 for $AR = 1$ and 10. For a given modified Rayleigh number $Ra^* \geqslant 10^4$, the lowest Nusselt number arises usually at the top heater and the highest Nusselt number is for the bottom heater.

Correlation

By means of the least-square regression analysis, the average Nusselt numbers, $(\overline{Nu}_h)_i$, $(i = 1\text{–}4)$, for each heater can be correlated well with the modified Rayleigh number and the aspect ratio of the enclosure of the following form:

$$(\overline{Nu}_h)_i = a_i(Ra^*)^{b_i}(AR)^{c_i} \tag{7}$$

where the coefficients a_i, b_i, and c_i are listed in Table 2 for $Ra^* = 10^4\text{–}10^6$ and $AR = 1\text{–}10$. The negative/

Table 2. Coefficients of equation (7)

i	a_i	b_i	c_i	Averaged deviation (%)	Correlation coefficient
1	1.459	0.194	−0.237	4.03	0.991
2	1.157	0.206	−0.241	3.83	0.990
3	1.049	0.202	−0.213	2.89	0.994
4	0.977	0.194	−0.188	2.87	0.994

positive values of the exponents for AR/Ra^* shown in the Table further asserts, respectively, the above-elaborated effects of the aspect ratio and the modified Rayleigh number on heat dissipation of the discrete heaters. The coefficient a_i in Table 2 showing a decreasing variation from the bottom heater ($i = 1$) to the top ($i = 4$) reflects the disparity between the Nusselt number of heaters. It is also interesting to note that the exponents of Ra^* in Table 2 appear to vary slightly between 0.194 and 0.206 with an average value of nearly 0.2 which is smaller than the exponent of 0.215 that is reported in ref. [9] for a correlation of the average Nusselt number vs Grashof number using the heater length as the characteristic length. Furthermore, a correlation for the dimensionless maximum surface temperature among the four discrete heaters has been developed vs the modified Rayleigh number and the aspect ratio as:

$$\theta_{h,max} = 0.962(Ra^*)^{-0.186}(AR)^{0.207} \quad (8)$$

for $Ra^* = 10^4$–10^7 and $AR = 1$–10 with an average deviation of 2.73% and a correlation coefficient of 0.997.

COMPARISON WITH EXPERIMENTS

Due to the limited size of the optics available in our holographic interferometry system, only a portion of the temperature field in the test cell could be mapped in the experiment. Figure 9 shows a comparison of the predicted temperature distribution with the holographic interferometric fringe pattern in the section between the second and third heater for $Ra^* = 3.2 \times 10^5$ and $AR = 10$. A favorable agreement is evidently observed between the predicted isotherms and the fringe distribution, thereby verifying the present simulation.

Shown in Figure 10 are the photograph of the flow pattern observed for $Ra^* = 4.0 \times 10^4$ and $AR = 10$ and the corresponding prediction of the streamline distribution. Apparently, the predicted multicellular structure in the core region is experimentally confirmed in the flow visualization.

Further comparison is made for the temperature distribution along the discretely heated vertical wall of the enclosure, as exemplified in Fig. 11 for $AR = 10$ at two different Ra^*. An examination of the figure reveals that the predicted temperatures at the discrete heaters compare quite well with the measured values of the embedded thermocouples. However, for the unheated sections between the heaters, there exists marked discrepancy between the prediction and measurement. This is primarily due to the wall-conduction effect in the discretely heated plate of the test cell.

CONCLUDING REMARKS

A combined numerical and experimental study has been presented to unveil primarily the effect of aspect ratio on the natural-convection air cooling of four discrete heaters in vertical rectangular enclosure. From the numerical simulations via a finite difference method, it has been found that contrary to the influence of increasing modified Rayleigh number, the increase of aspect ratio of the enclosure results in a substantial drop of heat dissipation from the discrete heaters, and thus in turn leads to significant rise of the heater surface temperature. The effect of enclosure aspect ratio on the average Nusselt number of the discrete heaters tends to degrade with the increase of the modified Rayleigh number. The maximum surface temperature arises usually at the top heater except for $Ra^* = 10^3$ where the hot spot is detected at the third heater. Temperature and flow fields of air inside the discretely heated enclosure of aspect ratio ten are,

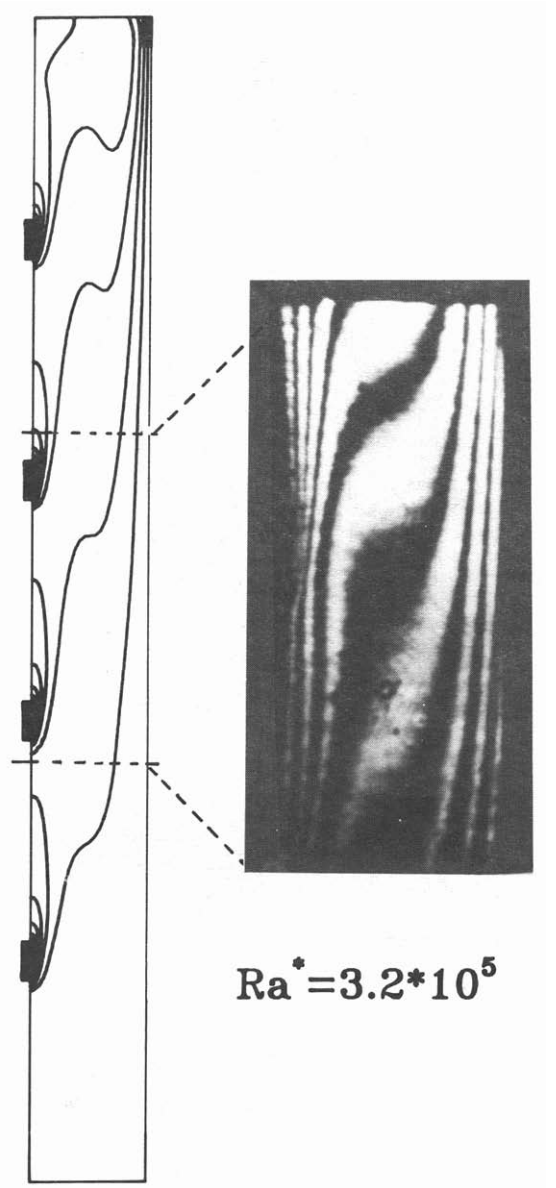

FIG. 9. Comparison of the predicted isotherms with the holographic interferometric fringes in the section between the second and third heater for $Ra^* = 3.2 \times 10^5$ and $AR = 10$.

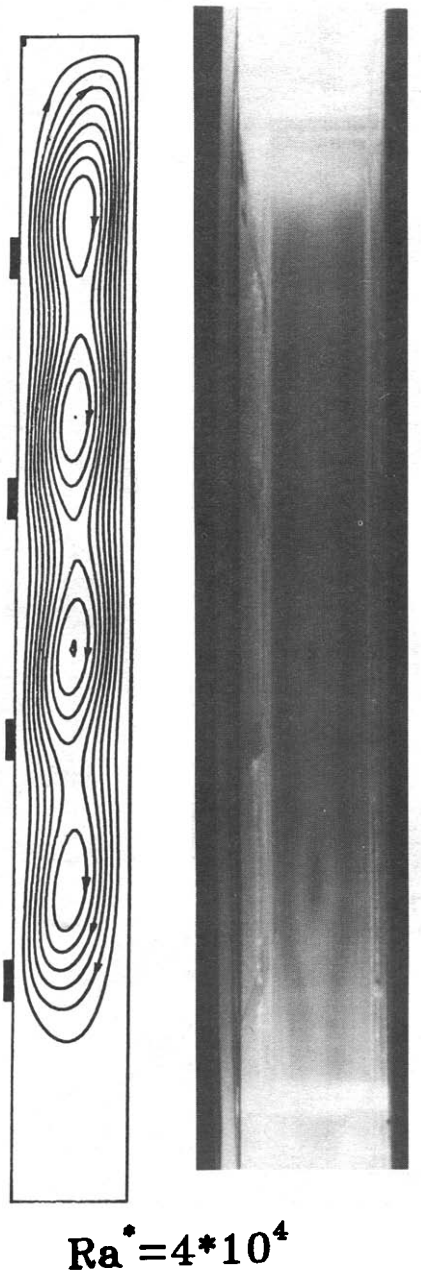

FIG. 10. Comparison of the predicted streamlines with the photograph of the flow visualization for $Ra^* = 4.0 \times 10^4$ and $AR = 10$.

respectively, found to agree well with the holographic interferometry fringe pattern and the smoke flow visualization. In particular, the multicellular core flow structure developed in an enclosure of $AR = 10$ at low modified Rayleigh number has been visualized experimentally. Furthermore, the predicted heater surface temperatures compare favorably with the measurement of thermocouples; but substantial discrepancy between the prediction and measurement exist for the temperature on the unheated sections. Based on the results obtained in the present work, the influences of other geometrical parameters, such as

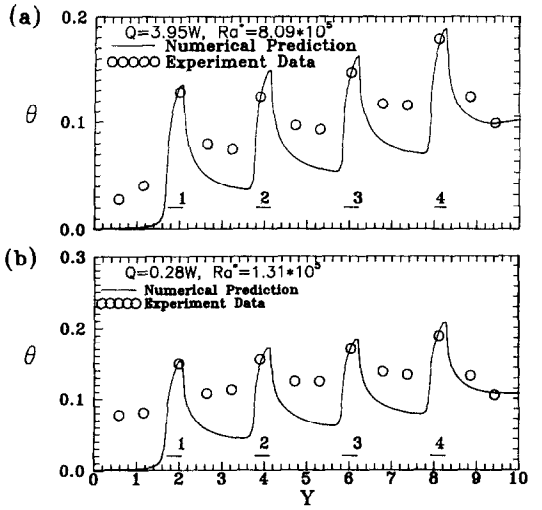

FIG. 11. Comparison of the predicted temperature distribution along the discretely heated wall with the measurement.

the relative heater size and placement, in a further wider range of modified Rayleigh number are topics for future studies.

Acknowledgement—The authors are very grateful to the support of the present study from National Science Council of the Republic of China through Grant No. NSC82-0401-E006-196.

REFERENCES

1. Y. Jaluria, Natural convection cooling of electronic equipment. In *Natural Convection: Fundamental and Applications* (Edited by S. Kakac *et al.*) pp. 961 986. Hemisphere, Washington, D.C. (1985).
2. F. P. Incropera, Convection heat transfer in electronic equipment cooling, *ASME J. Heat Transfer* **110,** 1097–1111 (1988).
3. H. H.-S. Chu, S. W. Churchill and C. V. S. Patterson, The effects of heaters size, location, aspect ratio, and boundary condition on two-dimensional, laminar natural convection in rectangular enclosure, *ASME J. Heat Transfer* **98,** 194–201 (1976).
4. K. Keyhani, V. Prasad and R. Cox, An experimental study of natural convection in a vertical cavity with discrete heat sources, *ASME J. Heat Transfer* **110,** 616 624 (1988).
5. M. Keyhani, V. Prasad, R. Shen and T. T. Wong, Free convection heat transfer from discrete heat sources in a vertical cavity. In *Natural and Mixed Convection in Electronic Equipment Cooling*, ASME HTD-Vol. 100, pp. 13–24 (1988).
6. R. Carmona and M. Keyhani, The cavity width effect on immersion cooling of discrete flush-heaters on one vertical wall of an enclosure cooled from the top, *ASME J. Electronic Packaging* **111,** 268–276 (1989).
7. V. Prasad, M. Keyhani and R. Shen, Free convection in a discretely heated vertical enclosure: effects of Prandtl number and cavity size, *ASME J. Electronic Packaging* **112,** 63–74 (1990).
8. G. Refai Ahmed and M. M. Yovanovich, Influence of discrete heat source location on natural convection heat transfer in a vertical square enclosure, *ASME J. Electronic Packaging* **113,** 268–274 (1991).
9. M. L. Chadwick, B. W. Webb and H. S. Heaton, Natural

convection from two-dimensional discrete heat sources in a rectangular enclosure, *Int. J. Heat Mass Transfer* **34,** 1679–1693 (1991).
10. M. D. Kelleher, R. H. Knock and K. T. Yang, Laminar natural convection in a rectangular enclosure due to a heated protrusion on one vertical wall—Part I: experimental investigation, *Proc. 2nd. ASME/JSME Thermal Engng. Joint Conf.*, Vol. 2, pp. 169–177 (1987).
11. L. Chen, M. Keyhani and D. R. Pitts, Convection heat transfer due to protruded heat sources in an enclosure, *AIAA J. Thermophys. Heat Transfer* **5,** 217–223 (1991).
12. J. J. Lee, K. V. Liu, K. T. Yang and M. D. Kelleher, Laminar natural convection in a rectangular enclosure due to a heated protrusion of one vertical wall—Part II: numerical simulations, *Proc. 2nd ASME/JSME Thermal Engng. Joint Conf.*, Vol. 2, pp. 179–185 (1987).
13. K. V. Liu, K. T. Yang and M. D. Kelleher, Three-dimensional natural convection cooling of an array of heated protrusions in an enclosure filled with dielectric fluid, *Proc. Int. Symposium on Cooling Technology for Electronic Equipment*, pp. 486–497 (1987).
14. C. J. Ho and J. Y. Chang, Conjugate natural-convection–conduction heat transfer in enclosures divided by horizontal fins, *Int. J. Heat Fluid Flow* **14,** 177–184 (1993).
15. G. de Vahl Davis, Natural convection of air in a square cavity: a benchmark solution, *Int. J. Numer. Methods Fluids* **3,** 249–264 (1983).
16. N. Ramman and S. A. Korpela, Multigrid solution of natural convection in vertical slot, *Numer. Heat Transfer A* **15,** 323–339 (1989).
17. C. J. Ho and Y. H. Lin, An experimental study of thermal-convection heat transfer in a horizontal concentric annulus partially filled with water, *Exp. Heat Transfer* **3,** 289–299 (1990).
18. S. J. Kline and F. A. McClintock, Describing uncertainties in single-sample experiments, *Mech. Engng* 3–12 (January 1953).